# Egyptian Journal of Chemistry

http://ejchem.journals.ekb.eg/

## Removal of Nickel and Cadmium from Aqueous Solution using Carbonaceous Magnesium Oxide: Thermodynamic and Kinetic study

**Saad Sh. Mohammed**

*Department of chemistry, College of science, University of Thi-Qar, Thi-Qar, Al Islah, Iraq,*

**Abstract**

Generation and entrance of toxic materials to aqueous environment causes many problems to human health. In the current study, the removal efficiency of Cd (II) and Ni(II) from aqueous solution was investigated by carbonaceous magnesium oxide. Three types of C-MgO adsorbents were synthesized via pyrolysis of prepared magnesium complex Mg(acac)$_2$ at three temperatures. Fabricated C-MgO adsorbents were characterized by XRD, SEM, and BET. XRD results revealed that the synthesized adsorbents consist of only magnesium oxide and carbon phase without any impurities. SEM technique used to characterizes the surface morphology of C-MgO samples. N2 adsorption-desorption isotherm used to calculate the BET surface area of prepared samples. The SEM results had a good agreement with BET measurement which improved that the high temperature increase the particles size and reduce the surface area. The adsorption studies showed that the carbonaceous magnesium oxides have good removal effeciency for Cd (II) and Ni(II) removal from aqueous solution and kinetically follow the pseudo-second order model.

Key words: Adsorption, Nanoparticles, Isotherm , Effeciency, Langmuir

## 1. Introduction

Metal ions removal, such as Cd, Pb, Ni, Hg, Cu, Co, Zn and Fe represent one of the important fields for environmental researchers [1-5]. Nickel (Ni) is an example of these heavy metal ions. Many industrial applications resources introduce it in the environment such as production of batteries and paints, mineral processing, manufacturing of sulfate, porcelain enameling and electroplating[6]. Hazardous of Nickel element is well known, it can cause gastrointestinal distress, lungs disorder severely and kidney damage [7]. Similarly, cadmium (Cd) is other example heavy metals, it can be introduce the environment via series of activities, such as metal plating, discharges from mining, plastic batteries, and paper industries [8].

Until now, different methods have been used to reduce water content from the heavy metals, such as membrane filtration, chemical precipitation, ion exchange, evaporation, ion exchange, reverse osmosis and electrodialysis [9–12]. However, among the various available efforts for removing of heavy metal from the aquatic environment is the adsorptive removal. Adsorption represents one of the referred and suitable methods due to its simplicity, a lower energy requirement, and absence the secondary waste products [13-14].The efficiency of any adsorption process mainly depends on the adsorbents capacity for adsorption. Materials with a large pore volume and high specific surface area are categorized as efficient adsorbents. The adsorbent large pore volume and high surface area facilitate the diffusion of mass and transport metal ions onto the adsorbent, thus enhancing the metal ion removal performance from the wastewater [15-16]. Metal oxides-carbon materials offer an important route for synthesizing new and improved functionalized materials with unique aspects of their components. Such materials have promising applications in catalysis, energy storage (super capacitors and batteries) and as adsorbents.

The inherent electronic conductivity and specific surface area of the most metal oxides will enhanced

_____

by the addition of carbon to these material.[17–26]. Different carbon forms, such as carbon spheres, activated carbon, carbon nanotubes,carbon fiber and grapheme have been utilized to synthesize metal oxide-carbon materials[ 27–34].

## 2.  Experimental
### 2.1 materials

Acetyleacetone, magnesium powder and toluene were purchased from Sigma Aldrich and used without further purification.

### 2. 2 Synthesis of carbonaceous magnesium oxide

Magnesium acetylacetonate Mg (acac)$_2$ was prepared via refluxing acetylacetone with magnesium metal. Then, the solvent and slurry were transferred to another flask to remove the solvent by decantation. The resulted complex washed with boiled toluene and evaporated until dryness. To prepare carbonaceous magnesium oxide, about 1 g of as-prepared magnesium complex subjected to pyrolysis at three different temperatures at 500, 600 and 700 ºC in quartz tube. The tube firstly evacuated and then filled with nitrogen gas to desired temperature and allowed to cool to room temperature naturally. Finally, the produced composite collected and washed with ethanol several times. The product labeled as C-MgO-500, C-MgO-600and C-MgO-700 where C refer to Carbonaceous and 500, 600 and 700 represent the pyrolysis temperatures.

### 2.3 Preparation of Ni$^{+2}$ and Cd$^{+2}$ Stock Solutions

Stock solution (1000 ppm ) for Cd$^{+2}$ and Ni$^{+2}$ were prepared by dissolving the cadmium chloride (NiCl$_2$) and nickel chloride (CdCl$_2$) in deionized water, respectively.

### 2.4 Removal experiments

To measure the removal efficiencies, 0.5 g of MgO-500 adsorbent added to Cd$^{+2}$ and Ni$^{+2}$ solutions (150, 250, 350, and 450 ppm) and stirred at 250 rpm for 2 h at 25 K. Then, solutions were filtrated and the concentrations of Cd$^{+2}$ and Ni$^{+2}$ measured by atomic absorption spectroscope (Varian AA240) to calculated the removal percentages.

### 2.5 kinetic experiments

Kinetic experiments were performed by adding 0.5 g of MgO-500 adsorbent to Cd$^{+2}$ and Ni$^{+2}$ solutions (25 mL, 150 ppm) and stirred at 250 rpm at 25 K for different time intervals (25, 50, 75, 100, 125, 150, 175, 200 and 225 min). After filtration, the concentration of to Cd$^{+2}$ and Ni$^{+2}$ in solutions were measured by atomic absorption spectroscope.

### 2.6 Characterization

The phase and pattern of prepared samples characterized by XRD(X-ray diffractometer, Panalytical, Model MPD) using CuK$\alpha$ radiation . SEM images crried out by (MIRA3, TESCAN-RMRC) (TM - 1000 ,Hitachi tabletop, Japan).The surface area of sythesized samples characterized by Nitrogen gas isotherm (adsorption-desorption) at 77K (Nova 2000, quantachrome, USA).

## 3. Results and discussion

The obtained XRD patterns of magnesium complex pyrolysis are shown in figure1. From figure 1, it can be seen that the XRD pattern of all samples display two characteristic peaks at 2theta 25.1 and 44.2 assigned to the carbon (100) and (101) planes respectively [[35].
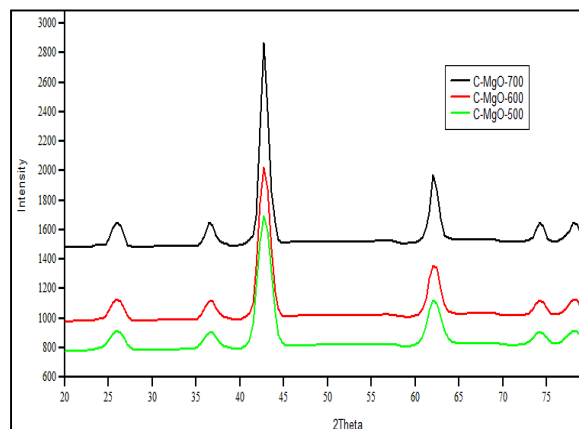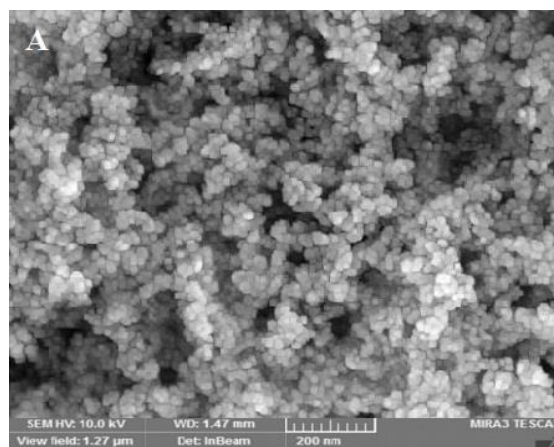
Fig.1 XRD patterns of C-MgO-500, C-MgO-600 and C-MgO-700

Also, the peaks belonged to the crystalline cubic structure of MgO appeared at 2 theta values 36.9, 42.8, 62.2 and 78.4 related to the (111), (200), (220) and (222) MgO planes respectively.
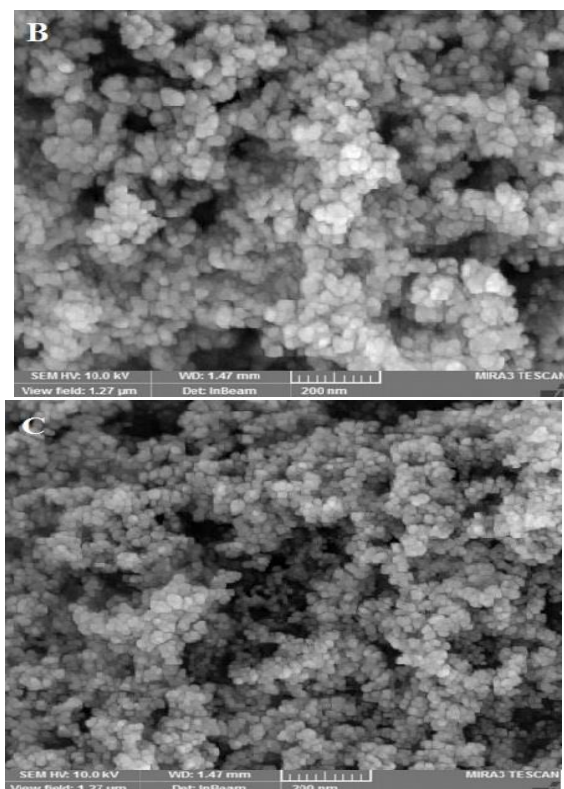
Fig.2 SEM images of (A) of C-MgO-500 (B)C-MgO-600 and (C) C-MgO-700

Figure 2(a-c) illustrate the SEM surface morphology micrographs related to the C- MgO composite. It can see that the surface of synthesized composites showed a small, ordered and spherical structure for all samples with about (15-25 nm) particle size . Also, there is an in increasing in the particles size at high pyrolysis temperatures due to gradual growth and aggregation of particles at high temperatures.
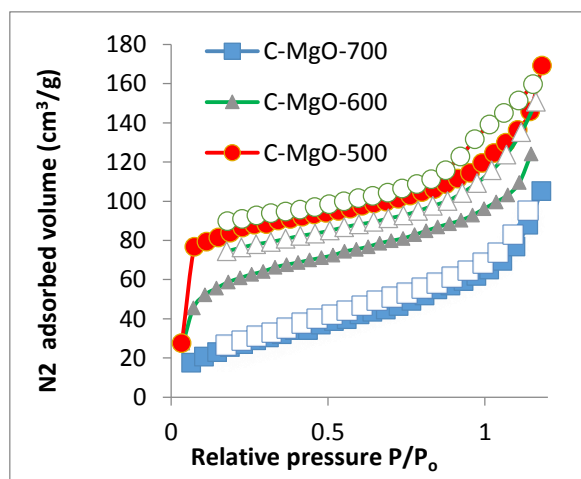


Figure 3: N2 adsorption isotherms of of C-MgO-500, C-MgO-600 and C-MgO-700

Figures 3 show the N$_2$ adsorption-desorption isotherms of prepared carbonaceous magnesium oxides at 77 K. The isotherms of the composites display typical IV type behavior according to (IUPAC classification) and the lower N$_2$ uptakes recorded at low pressure values.

The BET surface area of prepared samples were (329, 225 and 139 m$^2$. g$^{-1}$) for C-MgO-500, C-MgO-600 and C-MgO-700 respectively. However, it is obvious that rising the pyrolysis temperature significantly reduce the BET surface area in good agreement with SEM results which improved that the high temperature increase the particles size.

## 4. Adsorption studies
### 4.1 Batch Experiments

All the adsorption studies of Cd$^{+2}$ and Ni$^{+2}$ ions carried out by (C-MgO-500) which has the lager surface area therefore expected to showing better adsorption behavior. Technique of Batch equilibrium is used to evaluate the adsorption performance of C-MgO-500 adsorption toward Cd$^{+2}$ and Ni$^{+2}$ . Also, this method used to determine the effect of all control parameters. The removal efficiency and adsorption capacity were calculated using the following equations:

$$R\% = \frac{(C_0 - C_e)}{C_0} * 100$$

$$q_e = \frac{(C_0 - C_e)V}{m}$$

Where:

R% is the removal efficiency, q$_e$ is the adsorption capacity (mg/g), C$_o$ is the initial ions concentration (mg/L), Ce is the equilibrium ions concentrations (mg/L), V is the solution volume (L), and m is the weight of adsorbent(g).

### 4.2 Adsorption efficiency of Ni$^{+2}$ and Cd$^{+2}$ ions

The calculated removal efficiency of Cd$^{+2}$ and Ni$^{+2}$ ions from aqueous solution by C-MgO-500 are listed in table 1. As can be observed, the highest removal efficiencies recorded were 81.47% and 96.83% at 150 ppm Cd$^{+2}$ and Ni$^{+2}$ initial concentration, respectively. Also, there are gradually decreases in the removal efficiency as the concentration Cd$^{+2}$ and Ni$^{+2}$ increases attributed to the saturation of C-MgO-500 sites by the ions at high concentrations.

Table1. Removal efficiencies of Ni$^{+2}$ and Cd$^{+2}$ ions by C-MgO-500

| Concentration (ppm) | RE% of Cd$^{+2}$ | RE% of Ni$^{+2}$ |
|---|---|---|
| 150 | 96.83 | 81.47 |
| 250 | 95.92 | 80.29 |
| 350 | 94.33 | 73.64 |
| 450 | 92.84 | 53.45 |

### 4.3 Langmuir Adsorption Isotherm

Langmuir monolayer isotherm can be calculated by plotting the calculated equilibrium concentrations

_____

and adsorption capacities according to the following equation:

$$\frac{C_e}{q_e} = \left(\frac{1}{q_m}\right) * C_e + \left(\frac{1}{q_m K_L}\right)$$

Where, $C_e$ (mg $L^{-1}$) is the concentration of adsorbate at equilibrium, $q_e$ (mg $g^{-1}$) is the adsorbent adsorption capacity at equilibrium, $q_m$ (mg $g^{-1}$) is the adsorbent highest adsorption capacity and $K_L$ represent Langmuir constant.

The calculated Langmuir constants and Langmuir isotherms for $Cd^{+2}$ and $Ni^{+2}$ ions listed in table 2 and showed in figures (4-5).

Table 2 calculated Langmuir constants

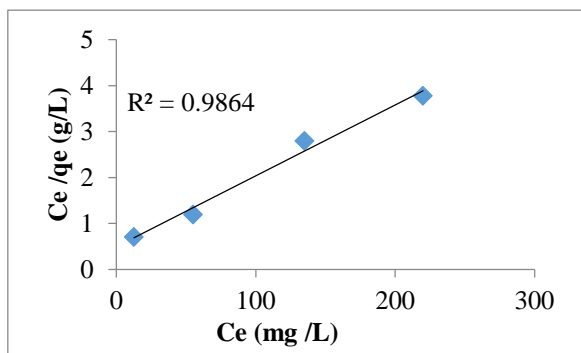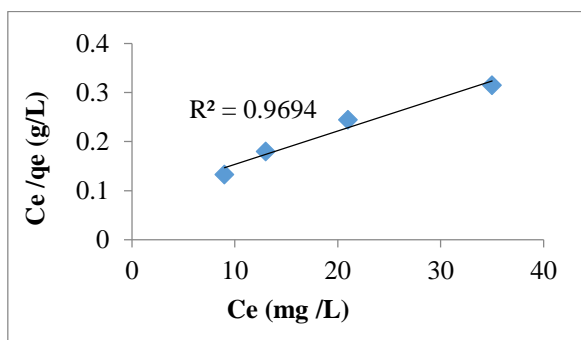| ion | $q_m$ (mg/g) | $K_L$ (L/g) | Regression $R^2$ |
|---|---|---|---|
| cadmium | 147.058 | 0.00058 | 0.96 |
| nickel | 64.935 | 0.00764 | 0.98 |



Fig.4 Langmuir isotherm of Nickel ions



Fig.5 Langmuir isotherm of Cadmium ions

Another important parameter is the separation factor $R_L$ which calculated according to the following equation:

$$R_L = \frac{1}{(1+(K_L C_o))}$$

Where, $C_o$ (mg/L) is the adsorbate initial concentration and $K_L$ (L/mg) is the Langmuir constant.

According to the results in table 3, the $R_L$ values lies between 0.919 and 0.225for both ions therapy the adsorption follow monolayer chemisorption.

Table3. Calculated $R_L$ values for Nickel and Cadmium ions

| $C_o$ (mg/L) | $R_L$ $Ni^{+2}$ (L/mg) | $R_L$ $Cd^{+2}$(L/mg) |
|---|---|---|
| 150 | 0.465 | 0.919 |
| 250 | 0.343 | 0.872 |
| 350 | 0.272 | 0.830 |
| 450 | 0.225 | 0.792 |

## 4.4 Freundlich Isotherm

Multi-layer adsorption can be described by Freundlich isotherm and calculated from the folloing equation:

$$\ln q_e = \left(\frac{1}{n}\right) \ln C_o + \ln K_F$$

Where, n and $K_F$ are the Freundlich constants.

As can be observed from $R^2$ values in table 3and figures (7-8), the adsorption of Cadmium ion by C-MgO-500 in good agreement with Freundlich isotherm compared with Nickel ion.

Also, the Freundlich positive and gradient constants values for both ions refer to multilayer adsorption of Ni and Cd ions onto the C-MgO-500.

According to the results that obtained from the two adsorption models, the Langmuir model is more suitable for adsorption Nickel ions while Freundlich model favorable for adsorption Cadmium ions. The results also reveal that the adsorption of nickel ions by C-MgO-500 is belonged to chemisorption process while the chemisorption and physisorption processes responsible for the adsorption of Cadmium ions.

Table4. Calculated Freundlich constants

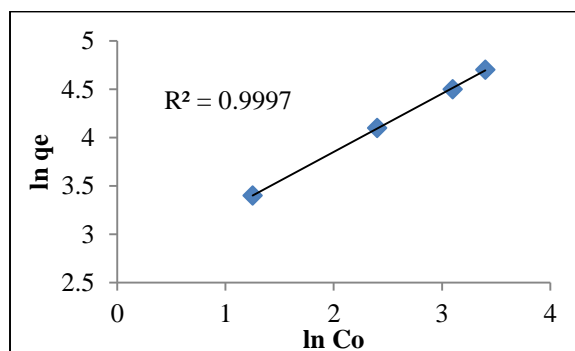| ion | 1/n (mg/g) | $K_F$(L/g) | $R^2$ |
|---|---|---|---|
| cadmium | 14.15 | 0.00058 | 0.99 |
| nickel | 13.32 | 0.00764 | 0.80 |



Fig. 7 Freundlich isotherm of Cadmium ions

_____

## 5. Kinetics Studies

Adsorption of Cadmium and Nickel ions by C-MgO-500 is monitored by pseudo-second order kinetic model and the results showed in figure 9 and summarized in table 4. Also, the adsorption capacity variation for both ions with time is plotted and showed in figure 8.

Table4. Psedo-second order parameters for adsorption Cd and Ni ions

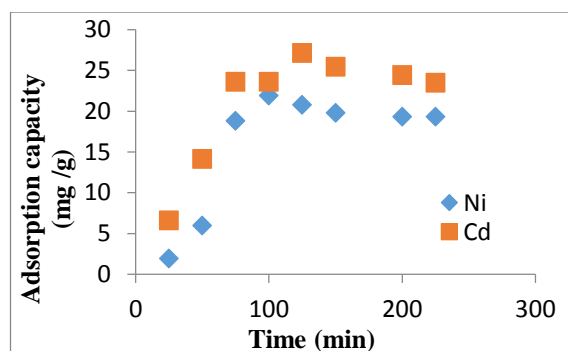| ion | $R^2$ | K (g mg$^{-1}$·min$^{-1}$) | Qe (mg g$^{-1}$) |
|-----|-------|------------------------------|--------------------|
| Ni | 0.9807 | 0.03393 | 0.773395 |
| Cd | 0.9912 | 0.0335 | 0.744491 |



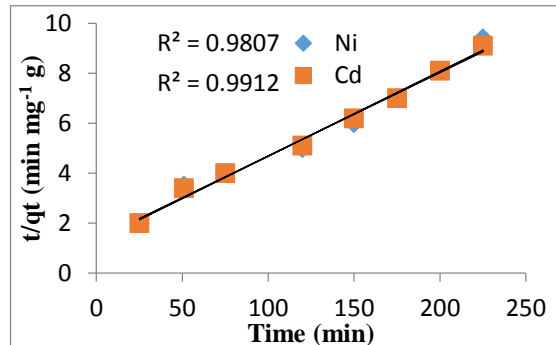Fig.8 Adsorption capacity of of Ni and Cd ions by C-MgO-500



Fig.9 Psedo-second order model of Ni and Cd ions

As can be noted from figure 9, the values of $R^2$ suggested that the pseudo-second order model is valid to describe the adsorption of Cd and Ni by C-MgO-500 adsorbent. The adsorption process of both ions can be occurred in two steps, the first including transfer of the soluble ions to the surface of C-MgO-500 sorbent, then diffusion of the adsorbed ions in the sorbents interior pores.

## 6. Conclusions

Carbonaceous magnesium oxide (C-MgO) has been successfully prepared using pyrolysis of Mg(acac)$_2$ complex at different temperatures. The

result of SEM technique reveals that the surface morphology of the C-MgO samples were small, ordered and spherical structure with (15-25 nm) particle size. The obtained XRD patterns of magnesium complex pyrolysis display the characteristic peaks of magnesium oxide and carbon. The results of BET showed The BET surface area of prepared samples were (329, 225 and 139 m$^2$·g$^{-1}$) for C-MgO-500, C-MgO-600 and C-MgO-700 respectively. Adsorption experiments results show the maximum removal efficiency of Cadmium ions by C-MgO adsorbent were 96.83% and 81.47% for Cadmium and Nickel ions respectively. Isotherms model results revealed that the Langmuir model is more suitable for adsorption Nickel ions by C-MgO-500 while Freundlich model favorable for adsorption Cadmium ions. The results also show that the adsorption of nickel ions by C-MgO-500 is belonged to chemisorption process while the chemisorption and physisorption processes responsible for the adsorption of Cadmium ions. The kinetic studies suggested that the pseudo-second order model is valid to describe the adsorption of Cadmium and Nickel ions by C-MgO-500 adsorbent.

## 7. References

[1] Thabet, W., Ahmed, S. B., Abdelwahab, O., & Soliman, N. F. (2020). Enhancement Adsorption of Lead and Cadmium Ions From Waste Solutions Using Chemically Modified Palmfibers. *Egyptian Journal of Chemistry*, *63*(12), 4917-4927.

[2] Elsehly, E. M. (2020). Enhanced removal of Ni (II) from aqueous solutions by effective acid functionalization of carbon nanotube based filters. *Egyptian Journal of Chemistry*, *63*(10), 3861-3871.

[3] Abd El Salam, H., & Sharara, T. (2019). A novel microwave synthesis of manganese based MOF for adsorptive of Cd (II), Pb (II) and Hg (II) ions from aqua medium. *Egyptian Journal of Chemistry*, *62*(5), 837-851.

[4] Duru, C., Nnabuchi, M., & Duru, I. (2019). Adsorption of Cu onto Maize Husk Lignocellulose in Single and Binary Cu-Zn Solution Systems: Equilibrium, Isotherm, Kinetic, Thermodynamic and Mechanistic Studies. *Egyptian Journal of Chemistry*, *62*(7), 1295-1305.

[5] Hassouna, M., Amin, R. R., Ahmed-Anwar, A. A., & Mahmoud, R. K. (2019). Efficient Removal of Oxytetracycline and Some Heavy Metals from Aqueous Solutions by Mg-Al Layered Double Hydroxide Nanomaterial. *Egyptian Journal of*

*Chemistry*, *62*(Special Issue (Part 1) Innovation in Chemistry), 177-195.

[6] Lakhdhar, I., Belosinschi, D., Mangin, P., & Chabot, B. (2016). Development of a bio-based sorbent media for the removal of nickel ions from aqueous solutions. Journal of environmental chemical engineering, 4(3), 3159-3169.

[7] Garg, U. K., Kaur, M. P., Garg, V. K., & Sud, D. (2008). Removal of nickel (II) from aqueous solution by adsorption on agricultural waste biomass using a response surface methodological approach. Bioresource technology, 99(5), 1325-1331.

[8] Cheung, C. W., Porter, J. F., & McKay, G. (2000). Elovich equation and modified second-order equation for sorption of cadmium ions onto bone char. Journal of Chemical Technology & Biotechnology, 75(11), 963-970.

[9] Esalah, J. O., Weber, M. E., & Vera, J. H. (2000). Removal of lead, cadmium and zinc from aqueous solutions by precipitation with sodium Di-(n-octyl) phosphinate. The Canadian Journal of Chemical Engineering, 78(5), 948-954.

[10] Abd Al-ameer, A. S., & Ali, S. A. (2020). Heavy metals determination and pre-concentration in river and drinking water samples at Nassiriyah City.

[11] Kumar, K. Y., Muralidhara, H. B., Nayaka, Y. A., Balasubramanyam, J., & Hanumanthappa, H. (2013). Hierarchically assembled mesoporous ZnO nanorods for the removal of lead and cadmium by using differential pulse anodic stripping voltammetric method. Powder technology, 239, 208-216.

[12] Mahmood, T., Saddique, M. T., Naeem, A., Mustafa, S., Dilara, B., & Raza, Z. A. (2011). Cation exchange removal of Cd from aqueous solution by NiO. Journal of Hazardous Materials, 185(2-3), 824-828.

[13] Zhu, J., Wei, S., Gu, H., Rapole, S. B., Wang, Q., Luo, Z., ... & Guo, Z. (2012). One-pot synthesis of magnetic graphene nanocomposites decorated with core@double-shell nanoparticles for fast chromium removal. Environmental science & technology, 46(2), 977-985.

[14] Jiang, M. Q., Jin, X. Y., Lu, X. Q., & Chen, Z. L. (2010). Adsorption of Pb (II), Cd (II), Ni (II) and Cu (II) onto natural kaolinite clay. Desalination, 252(1-3), 33-39.

[15] Ali, I. (2012). New generation adsorbents for water treatment. Chemical reviews, 112(10), 5073-5091.

[16] Khajeh, M., Laurent, S., & Dastafkan, K. (2013). Nanoadsorbents: classification, preparation, and applications (with emphasis on aqueous media). Chemical reviews, 113(10), 7728-7768.

[17] Mishra, A. K., & Ramaprabhu, S. (2011). Functionalized graphene-based nanocomposites for supercapacitor application. The Journal of Physical Chemistry C, 115(29), 14006-14013.

[18] Zhi, M., Xiang, C., Li, J., Li, M., & Wu, N. (2013). Nanostructured carbon–metal oxide composite electrodes for supercapacitors: a review. Nanoscale, 5(1), 72-88.

[19] Chou, S. L., Lu, L., Wang, J. Z., Rahman, M. M., Zhong, C., & Liu, H. K. (2011). The compatibility of transition metal oxide/carbon composite anode and ionic liquid electrolyte for the lithium-ion battery. Journal of Applied Electrochemistry, 41(11), 1261.

[20] Zhao, X., Xia, D., & Zheng, K. (2012). Fe3O4/Fe/carbon composite and its application as anode material for lithium-ion batteries. ACS applied materials & interfaces, 4(3), 1350-1356.

[21] Li, J., Ai, Z., & Zhang, L. (2009). Design of a neutral electro-Fenton system with Fe@Fe2O3/ACF composite cathode for wastewater treatment. Journal of hazardous materials, 164(1), 18-25.

[22] Li, Y., Meng, Q., Zhu, S. M., Sun, Z. H., Yang, H., Chen, Z. X., ... & Zhang, D. (2015). A Fe/Fe 3 O 4/N-carbon composite with hierarchical porous structure and in situ formed N-doped graphene-like layers for high-performance lithium ion batteries. Dalton Transactions, 44(10), 4594-4600.

[23] Busch, M., Schmidt, W., Migunov, V., Beckel, A., Notthoff, C., Kompch, A., ... & Atakan, B. (2014). Effect of preparation of iron-infiltrated activated carbon catalysts on nitrogen oxide conversion at low temperature. Applied Catalysis B: Environmental, 160, 641-650.

[24] Bhunia, P., Kim, G., Baik, C., & Lee, H. (2012). A strategically designed porous iron–iron oxide matrix on graphene for heavy metal adsorption. Chemical Communications, 48(79), 9888-9890.

[25] Wang, T., Peng, Z., Wang, Y., Tang, J., & Zheng, G. (2013). MnO nanoparticle@ mesoporous carbon composites grown on conducting substrates featuring high-performance lithium-ion battery, supercapacitor and sensor. Scientific reports, 3(1), 1-9.

[26] Wang, G., Zhang, L., & Zhang, J. (2012). A review of electrode materials for electrochemical supercapacitors. Chemical Society Reviews, 41(2), 797-828.

[27] AbdulAlmohsin, S. M., Khedhair, A. A., & Ajeel, S. K. (2019). Facile Synthesis of Polyaniline-Single Wall Carbon Nanotube Nanocomposite as Hole Transport Material and Zinc Oxide Nanorodes as Metal Oxide to Integration Solid-State Dye-sensitized Solar Cells. University of Thi-Qar Journal, 14(2), 1-13.

[28] Al-Janabi, R. A. S. M. (2018). The Effect of Tempering Heat Treatment on Some Mechanical Properties of Medium Carbon Steel (AISI 1045) Formed By Cold Forging Process. University of Thi-Qar Journal, 13(3), 70-80.

[29] Hu, C., Lu, T., Chen, F., & Zhang, R. (2013). A brief review of graphene–metal oxide composites synthesis and applications in photocatalysis. Journal of the Chinese Advanced Materials Society, 1(1), 21-39.

[30] Erabeea, I. K., Ahsanb, A., Imteazc, M., & Alomd, M. M. (2019). Adsorption of hexavalent chromium using activated carbon prepared from garden wastes. DESALINATION AND WATER TREATMENT, 164, 293-299.

[31] Kim, D. W., Rhee, K. Y., & Park, S. J. (2012). Synthesis of activated carbon nanotube/copper oxide composites and their electrochemical performance. Journal of alloys and compounds, 530, 6-10.

[32] Arod, P., & Shivashankar, S. A. (2016). Synthesis of unique metal oxide/carbon composites via sealed-tube pyrolysis of metal acetylacetonates and the mechanism of their formation. RSC advances, 6(70), 65366-65372.

[33] Liu, H. J., Bo, S. H., Cui, W. J., Li, F., Wang, C. X., & Xia, Y. Y. (2008). Nano-sized cobalt oxide/mesoporous carbon sphere composites as negative electrode material for lithium-ion batteries. Electrochimica Acta, 53(22), 6497-6503.

[34] Xu, J., Wang, K., Zu, S. Z., Han, B. H., & Wei, Z. (2010). Hierarchical nanocomposites of polyaniline nanowire arrays on graphene oxide sheets with synergistic effect for energy storage. ACS nano, 4(9), 5019-5026.

[35] Zhang, L., Su, Z., Jiang, F., Yang, L., Qian, J., Zhou, Y., ... & Hong, M. (2014). Highly graphitized nitrogen-doped porous carbon nanopolyhedra derived from ZIF-8 nanocrystals as efficient electrocatalysts for oxygen reduction reactions. *Nanoscale*, 6(12), 6590-6602.

## 8. Arabic Abstract

يتسبب توليد المواد السامة ودخولها إلى البيئة المائية في حدوث العديد من المشاكل لصحة الإنسان. في الدراسة الحالية ، تم اختبار كفاءة أوكسيد الماغنسيوم الكربوني لإزالة ايون الكادميوم (II) وايون النيكل (II) من المحلول المائي. تضمنت الدراسة تحضير ثلاثة أنواع من المادة المازة (اوكسيد المغنسيوم الكربوني) عند ثلاث درجات حرارية بواسطة التحلل الحراري لمركب (مغنسيوم اسيتايل اسيتونات) المحضر. تم فحص المواد المازة المحضرة بواسطة طيف حيود الاشعة السينية, المجهر الالكتروني الماسح وفحص المساحة السطحية. أظهرت نتائج حيود الاشعة السينية أن المواد المحضرة تتكون فقط من أوكسيد المغنيسيوم الكربوني بدون أي شوائب اخرى. فحوصات المساحة السطحية للمركبات المحضرة اجريت بواسطة امتزاز غاز النيتروجين وكانت متوافقة جيداً مع قياسات المجهر الالكتروني الماسح التي اشارت الى ان ارتفاع درجة الحرارة تؤدي إلى زيادة حجم الجسيمات وبالتالي تقليل مساحة السطح. أظهرت دراسات الامتزاز أن أكاسيد المغنيسيوم الكربوني المحضرة تمتلك كفاءة ازالة جيدة لأيونات الكادميوم (II) والنيكل (II) من المحلول المائي وحركية الامتزاز تتبع نموذج الرتبة الثانية الكاذبة.